Journal of AppliedMath 2024, 2(5), 1807.
https://doi.org/10.59400/jam1807

Article

Mathematical modelling of dengue fever transmission dynamics in Kenya

Brian Nyanaro[1,*], George Kimathi[2], Mary Wainaina[1]

[1] Department of Mathematics and Actuarial Science, Catholic University of Eastern Africa, Nairobi Box 62157-00200, Kenya

[2] School of Computing and Information Technology, University of Kigali, Kigali 101, Rwanda

*** Corresponding author:** Brian Nyanaro, brian.nyanaro@gmail.com

CITATION

Nyanaro B, Kimathi G, Wainaina M. Mathematical modelling of dengue fever transmission dynamics in Kenya. Journal of AppliedMath. 2024; 2(5): 1807. https://doi.org/10.59400/jam1807

ARTICLE INFO

Received: 30 September 2024
Accepted: 19 November 2024
Available online: 17 December 2024

Abstract: Dengue fever is one of the diseases emerging in Kenya due to effects of climate change and urbanization. The disease is caused by a family of four flavivirus serotypes DENV 1 to DENV4. A deterministic compartmental model for the dengue fever spread dynamics was developed and utilized to examine dengue fever spread dynamics in Kenya. The model was established to be well-stated mathematically and epidemiologically well-posed through positivity and boundedness analysis. The dengue-free equilibrium state was determined as part of the solution to the system of differential equations defining the spread dynamics. The basic reproduction number was determined through the next-generation matrix and used to confirm the stability of the steady state determined before. The study found that when the basic reproduction number was greater than one, the dengue endemic state dominated the solution of the spread dynamics, while when the basic reproduction number was less than one, the dengue free state dominated the solution, implying the disease died down progressively. Sensitivity analysis of the basic reproduction number was carried out to determine the candidate parameters for an optimal control solution. The study found that the infection rate of susceptible mosquitoes, the survival rate of pre-adult mosquitoes, the natural death rate of mosquitoes, the rate at which mosquito survived the extrinsic incubation stage, and the egg-laying of mosquitoes were the most sensitive parameters of the model.

Keywords: basic reproductive number; dengue fever; equilibrium points; mathematical modelling; numerical simulations

1. Introduction

Dengue fever is one of the most common mosquito-borne diseases that is posing a major public health threat especially in urban and semi-urban areas. It is an emerging vector-borne disease caused by the dengue virus that has been increasing progressively in the last 40 years. The increase is attributed to the expansion of both the virus and the mosquitoes in the tropics and subtropic regions [1]. The virus is consist of a family of four flavivirus serotypes: DENV 1, DENV 2, DENV 3 and DENV 4, which are antigenically specific but firmly related [2]. The disease has colonised urban and semi-urban centers in the subtropical and tropical climatic regions across the globe. The disease burden is felt more in the Americas, Eastern Mediterranean, Southeast Asia, Africa and the West Pacific regions [3]. About 70% of the disease burden is felt in the continent of Asia [4]. However, most countries across the globe are at risk of an epidemic from dengue fever, with more than 100 countries at risk. It is the second deadliest mosquito-borne disease after Malaria, with thousands of fatalities globally and over 390 million infections across the globe. The clinically manifested cases are

approximately 25%, translating to about 96 million cases [5].

Additionally, about half of the global human inhabitants live in places that predispose them to high susceptibility to dengue fever. The *Aedea Aegypi* mosquitoes that are mainly responsible for the spread of dengue fever are temporal-specific. They thrive in the tropical and subtropical urban and peri-urban centers of the world. Their existence is further boosted by emerging issues such as climate change. In particular, climate change has led to an increase in temperature, leading to more favourable conditions for the dengue fever endemic intensity to thrive.

The dengue virus is spread by mosquitoes, more especially the *Aedes Aegyti* mosquitoes. It belongs to the same family as other flaviviruses, such as Omsk haemorrhage fever, West Nile virus, Kyasanur forest virus, and yellow fever [6]. Dengue fever is known to cause mortality and mild morbidity, but generally, the infected individuals recover within two weeks from the onset of the fever. Recovered individuals attain permanent immunity from the strain they have recovered from [7]. However, some individuals develop more severe illnesses, such as dengue shock syndrome (DSS) and dengue haemorrhagic fever (DHF), which are more morbid [8]. These two forms are life-threatening conditions associated with dengue fever infection where DHF is associated with thrombocytopenia and haemorrhage while DSS is characterised by excessive plasma leakage. As a consequence, of the two conditions, dengue fever has an average case fatality of 5% [9].

In the last ten years, various vaccines have progressed through different development stages, with some in the clinical trials stage [10] in both endemic and non-endemic areas. One of the most progressive vaccines is the live-attenuated vaccine, Dengvaxia, which has been incensed in several countries. However, the initial reviews have shown that it has low efficacy in children and individuals who have never contracted dengue fever before. On the other hand, it has been shown to lead to severe sickness for people who have no history of exposure before [11]. As such, control measures of dengue fever are dependent on control measures that target vector control as opposed to vaccines [12].

2. Dengue fever in Kenya

The first ever case of dengue fever (DF) recorded in Kenya was identified in a Canadian tourist in 1982 in the coastal town of Malindi [13, 14]. It was attributed to the DENV-2 serotype, which was again isolated in 1997 in Kilifi County. There were several reported outbreaks between 2011 and 2014 in the coastal towns and in the Northeastern counties, specifically in Mandera county, mostly among officers serving the AMISOM (African Mission Soldiers in Somalia) [15].

These outbreaks can be summarised geospatially by the geographical map of Kenya with the outbreak points as shoen in the **Figure 1** below.

These later outbreaks were attributed to the other remaining serotypes of DENV-1, DENV-2, and DENV-3. An outbreak involving DENV-2 was reported between 2014 and 2015 in Kilifi County, and later in 2017 the same cosmopolitan serotype caused another outbreak within Malindi town in Kilifi county [16, 17]. The cosmopolitan DENV-2 dominated outbreaks in 2017 with another outbreak in North Eastern Kenya.

Later the DENV-4 serotype was reported in Busia county opening a new chapter of the spread of DENV in the highland region of the country. The epidemiology of dengue fever in East Africa and Africa is little understood compared to other tropical areas of the globe [18]. The spatial distribution of the serotype within the country remains unaccounted for and more research is needed to establish the geographical distribution of the serotype and the enabling spatial factors. Some of the factors could be limited surveillance of the disease, limited diagnostics specific to dengue fever, and limited expertise awareness of the disease by clinicians in the non-coastal regions of the country [17].

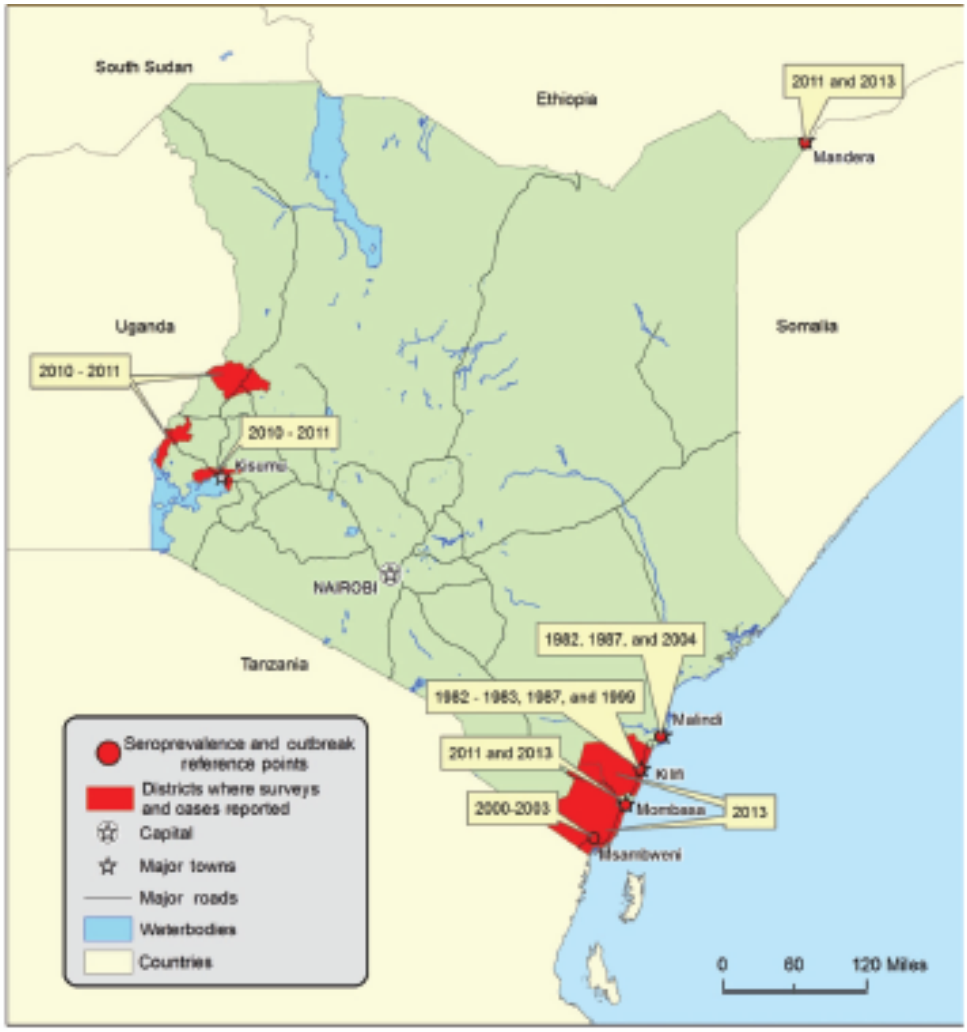

Figure 1. Map of outbreaks and seroprevalence od dengue fever in Kenya [16].

In the recent past, dengue fever outbreaks have become annual outcomes due to various factors affecting the coastal region. Such multifactorial contributing factors include increased population growth, increased urbanization, increased rapid movement of people from place to place, and climate change that favours increased activity of *Aedes Aegyti* and *Aedes albopictus*. The *Aedes Aegyti* and *Aedes albopictus* are the principal mosquitoes responsible for the spread dengue fever in countries around the Indian Ocean [17].

The first reported cases of the latest outbreak of dengue fever were documented

in January 2021 in the coastal counties of Lamu and Mombasa. The initial cases had ballooned in Lamu County by April of the same year, indicating a high transmission rate of about 51% of the targeted sample of the community. Immediate interventions were sought from the Red Cross Society through the Medical Services and Public Health Department of the county government of Lamu. Cases were on the rise in both counties, necessitating public health awareness across the two counties with more focus on Mvita sub-county, which accounted for a majority of the reported cases. However, the reported cases are not a true reflection of the transmission dynamics due to the high number of unreported cases and misdiagnoses that could have occurred [17].

Studies on dengue fever spread dynamics have been considered by various studies to investigate the trends of dengue fever in the population. For instance Asamoah et al., discussed the analysis for dengue virus infection model, focusing on a model that incorporated partial immune individuals and asymptomatic individuals. Their work incorporated the partial immune class and the carrier (asymptomatic) class, which accounts for partial immunity acquired from vaccination or recovery from one serotype of the dengue virus [19]. The study utilised mathematical modelling as a tool for investigating the spread dynamics with the objective of conducting optimal control analysis. As such, this study is based on similar foundations aimed at investigating the spread of dengue fever dynamics in Kenya as an emerging disease catalysed by climate change.

This study employs the powerful tool of mathematical modelling for strategic preparedness of disease outbreaks. As such, it will provide fundamental information necessary for development of interventions to curb and contain outbreaks of dengue fever in Kenya. In particular, the findings and recommendations of the study will resource allocation and research in the dengue fever spread dynamics. Furthermore, the information will provide insights into the dengue fever spread dynamics, introduce a combination of novel control strategies that are aligned with modern challenges [20].

In addition, the study will provide a link between scientific and public health policy making, which will lead to evidence-based policy that ensure the well-being of members of the community. It will also provide guidance to the necessary steps that can be taken to prevent dengue fever from being endemic in Kenya by utilizing the available data to give simulations at a lower cost than when addressing an outbreak.

3. Model description and formulation

The model is divided into two broad subpopulations of vectors (Female *Aedes egypti* mosquitoes) and human beings. The Female *Aedes egypti* mosquitoes will be divided into sub-populations as follows: Aquatic phase mosquitoes (eggs, larva, and pupa) $(L(t))$, Susceptible mosquitoes $(S_v(t))$, Exposed mosquitoes $(E_v(t))$, and Infectious mosquitoes $(I_v(t))$. The Exposed compartment contains all mosquitoes that have been infected with dengue virus but are in the latent stage, where they are not infectious yet. Once a mosquito is infected with the dengue virus, it does not recover from it; it dies with the virus. The total population of the vectors is given by

$$N_v = L(t) + S_v(t) + E_v(t) + I_v(t)$$

The human subpopulation constitutes the following compartments: The Susceptible humans $(S_h(t))$, the exposed humans $(E_h(t))$, the infectious humans $(I_h(t))$, and the recovered $(R_h(t))$. The exposed humans are individuals already infected with dengue fever but in the latent stage before they become infectious. The recovered humans $(R_h(t))$ obtain temporary immunity from the serotype they have recovered from and a temporary immunity from the other three serotypes. The total population of the human beings is given by

$$N_h = S(t)_h + E_h(t) + I_h(t) + R_h(t)$$

3.1. Model formulation

The model subpopulations and their corresponding homogenous compartments are illustrated by the **Figure 2** below:

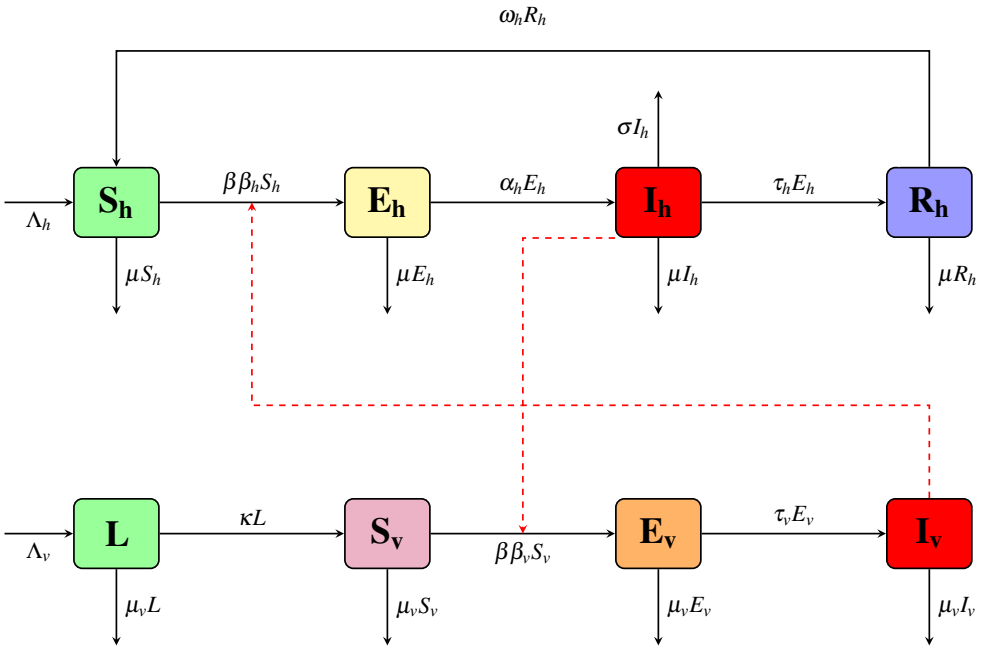

Figure 2. Dengue fever transmission dynamics model encompassing human and mosquito populations.

The pace of advancement from one compartment to another is quantified by the model parameters, which represent the illness development dynamics. The recruitment rate of the human subpopulation is denoted by Λ_h and it encompasses the natural birth rate as the dominating contributor. The recovery rate of human beings from one serotype is represented by τ_h, while the rate at which human temporary immunity wanes is represented by ω_h. The rate of infection of susceptible humans is represented by β_h, while the rate of human beings moving from the intrinsic incubation phase to the infectious phase is represented by α_h, while the natural death rate of human beings is represented by μ_h. Lastly, σ_h represents the disease-induced death. On the vector subpopulation, τ_v represents the rate at which vectors leave the extrinsic latent stage to become infectious. The egg-laying rate of *Aedes aegypti*, which dominates the

recruitment rate of vector, is represented by Λ_v, while the survival rate of mosquitoes during the transition from pre-larvae to adults is represented by κ. β_v represents the infection rate of susceptible mosquitoes while the natural death rate of *Aedes aegypti* mosquitoes is represented by μ_v. A summary of the parameters that were considered for the study is presented in **Table 1** below.

Table 1. A summary of parameter description, their values and sources.

Parameter	Description	Value (per day)	Source
Λ_h	Human recruitment rate.	1538	[21]
τ_h	Human recovery rate.	0.154	[22]
ω_h	Immunity waning rate of humans.	0.1	Estimated
β_h	Infection rate of the susceptible Humans	4.8×10^{-8}	[19]
α_h	Rate of humans moving from latent stage to infectious stage.	0.12	[22]
σ_h	Dengue fever mortality rate	0.01969	[21]
μ_h	Natural death rate of humans.	0.0138214021	Calculated
τ_v	Rate of mosquitoes moving from latent stage to infectious stage	0.1	
Λ_v	Egg-laying rates of *Aedes aegypti* mosquitoes.	2938	[21]
κ	Survival rates of mosquitoes at the pre-development stage.	0.19	[22]
β_v	Infection rate of susceptible mosquitoes.	1×10^{-5}	[19]
μ_v	Natural death rate of *Aedes aegypti* mosquitoes.	0.0323	[22]

3.2. Model equations

The model description in **Figure 2** above gives rise to a system of non-linear differential equations below that describe the dengue fever disease host-vector transmission dynamics.

$$\begin{cases} \frac{dS_h}{dt} = \Lambda_h - (\beta\,\beta_h + \mu_h) S_h + \omega_h R_h \\ \frac{dE_h}{dt} = \beta\,\beta_h S_h - (\alpha_h + \mu_h) E_h \\ \frac{dI_h}{dt} = \alpha_h E_h - (\tau_h + \mu_h + \sigma_h) I_h \\ \frac{dR_h}{dt} = \tau_h I_h - (\omega_h + \mu_h) R_h \\ \frac{dL}{dt} = \Lambda_v - (\kappa + \mu_v) L \\ \frac{dS_v}{dt} = \kappa L - (\beta\,\beta_v + \mu_v) S_v \\ \frac{dE_v}{dt} = \beta\,\beta_v S_v - (\tau_v + \mu_v) E_v \\ \frac{dI_v}{dt} = \tau_v E_v - \mu_v I_v \end{cases} \tag{1}$$

with the initial conditions

$$S_h(0) \geqslant 0, E_h(0) \geqslant 0, I_h(0) \geqslant 0, R_h(0) \geqslant 0 \tag{2}$$

$$S_v(0) \geqslant 0, E_v(0) \geqslant 0, I_v(0) \geqslant 0, R_v(0) \geqslant 0 \tag{3}$$

4. Basic properties of the model

In this section, we study the posedness of the epidemiological model as stated by investigating the positivity and invariant region span by the model.

4.1. The invariant region

Theorem 1. *Let* $\Phi = \{(S_h(t), E_h(t), I_h(t), R_h(t), L(t), S_v(t), E_v(t), I_v(t)) \in \mathbb{R}_+^8 : (S_h(0), E_h(0),\ I_h(0), R_h(0), L(0), S_v(0), E_v(0), I_v(0)) \geqslant 0\}$ *therefore the solutions of* $\{(S_h(t), E_h(t), I_h(t),\ R_h(t), L(t), S_v(t), E_v(t), I_v(t))\}$ *are non-negative at all time* $t \geqslant 0$.

Proof. The total human population at any given time is equal to $N_h(t) = S_h(t) + E_h(t) + I_h(t) + R_h(t)$; therefore, after differentiating both sides of the equation we obtained :

$$\frac{dN_h(t)}{dt} = \frac{dS_h(t)}{dt} + \frac{dE_h(t)}{dt} + \frac{dI_h(t)}{dt} + \frac{dR_h(t)}{dt}$$

which yields the result

$$\frac{dN_h(t)}{dt} = \Lambda_h - \mu_h S_h - \mu_h E_h - \mu_h I_h - \sigma_h I_h - \mu_h R_h \tag{4}$$

In the absence of death induced by dengue fever, the Equation (4) can be written as

$$\frac{dN_h(t)}{dt} \leq \Lambda_h - \mu_h S_h - \mu_h E_h - \mu_h I_h - \mu_h R_h$$

which can be reduced to

$$\frac{dN_h(t)}{dt} \leq \Lambda_h - \mu_h N_h(t) \tag{5}$$

solving the differential inequality in Equation (5)

$$N_h(t) \leqslant \frac{\Lambda_h}{\mu_h} - \left(\frac{\Lambda_h - \mu_h N_h(0)}{\mu_h}\right) e^{-\mu_h t}$$

As $t \to \infty$ the total human population N_h converges to $\dfrac{\Lambda_h}{\mu_h}$.

As a consequence, $0 \leqslant N_h \leqslant \dfrac{\Lambda_h}{\mu_h}$. It follows that if $N_0 \leqslant \dfrac{\Lambda_h}{\mu_h}$ then $N_t \leqslant \dfrac{\Lambda_h}{\mu_h}$. As a result,

$$\Phi_h = \left\{(S_h(t), E_h(t), I_h(t), R_h(t)) \in \mathbb{R}_+^4 : S_h(t) + E_h(t) + I_h(t) + R_h(t) \leqslant \frac{\Lambda_h}{\mu_h}\right\} \tag{6}$$

Similarly, the total vector population of dengue fever is described by $N_v = L(t) +$

$S_v(t)+E_v(t)+I_v(t)$ thus

$$\frac{dN_v(t)}{dt}=\frac{dL(t)}{dt}+\frac{dS_v(t)}{dt}+\frac{dE_v(t)}{dt}+\frac{dI_v(t)}{dt}$$

which simplifies to

$$\frac{dN_v(t)}{dt}\leqslant \Lambda_v-\mu_v N_v(t) \tag{7}$$

Upon solving Equation (7) a solution of the form,

$$N_v(t)\leqslant \frac{\Lambda_v}{\mu_v}-\left(\frac{\Lambda_v-\mu_v N_v(0)}{\mu_v}\right)e^{-\mu_v t} \tag{8}$$

is obtained.

Therefore, from Equation (8), as $t\to\infty$ the vector population N_v converges to $\frac{\Lambda_v}{\mu_v}$ that is $\left(N_v\to\frac{\Lambda_v}{\mu_v}\right)$. Therefore, $0\leqslant N_v\leqslant\frac{\Lambda_v}{\mu_v}$. As a result, if $N_0\leqslant\frac{\Lambda_v}{\mu_v}$ then it follows $N_v(t)\leqslant\frac{\Lambda_v}{\mu_v}$. On this basis, we had

$$\Phi_v=\left\{(L(t),S_v(t),E_v(t),I_v(t))\in\mathbb{R}^4_+ : L(t)+S_v(t)+E_v(t)+R_v(t)\leqslant\frac{\Lambda_v}{\mu_v}\right\} \tag{9}$$

In conclusion, the feasible region for the nonlinear system of differential Equation (1) is given by

$$\Phi=\Phi_h\times\Phi_v\subset\mathbb{R}^4_+\times\mathbb{R}^4_+ \tag{10}$$

where Φ_h and Φ_v are defined as

$$\Phi_h=\left\{(S_h(t),E_h(t),I_h(t),R_h(t))\in\mathbb{R}^4_+ : S_h(t)+E_h(t)+I_h(t)+R_h(t)\leqslant\frac{\Lambda_h}{\mu_h}\right\} \tag{11}$$

and

$$\Phi_v=\left\{(L(t),S_v(t),E_v(t),I_v(t))\in\mathbb{R}^4_+ : L(t)+S_v(t)+E_v(t)+R_v(t)\leqslant\frac{\Lambda_v}{\mu_v}\right\} \tag{12}$$

where Φ is a positively invariant region, as a result the models, as constituted is well-posed and epidemiologically well stated for analysis.□

4.2. Positivity of the solutions

In this subsection, the necessary criteria for which the solutions to the system of differential Equation (1) remain positive are discussed. It is necessary for the solutions for both the human population and mosquito population to remain positive for the model to remain well-stated and well-posed.

Theorem 2. *Each solution of the system of differential Equation (1) governed by the initial conditions 2 and 3 is non-negative; that is, it exists in the interval* $[0,\infty]$ *for all* $t\geqslant 0$.

Proof. Let's consider the system of differential Equations (1) written below as

$$\frac{dS_h}{dt} = \Lambda_h - (\beta\,\beta_h + \mu_h)\,S_h + \omega_h R_h \tag{13}$$

$$\frac{dE_h}{dt} = \beta\,\beta_h\,S_h - (\alpha_h + \mu_h)\,E_h \tag{14}$$

$$\frac{dI_h}{dt} = \alpha_h\,E_h - (\tau_h + \mu_h + \sigma_h)\,I_h \tag{15}$$

$$\frac{dR_h}{dt} = \tau_h\,I_h - (\omega_h + \mu_h)\,R_h \tag{16}$$

$$\frac{dL}{dt} = \Lambda_v - (\kappa + \mu_v)\,L \tag{17}$$

$$\frac{dS_v}{dt} = \kappa L - (\beta\,\beta_v + \mu_v)\,S_v \tag{18}$$

$$\frac{dE_v}{dt} = \beta\,\beta_v\,S_v - (\tau_v + \mu_v)\,E_v \tag{19}$$

$$\frac{dI_v}{dt} = \tau_v\,E_v - \mu_v\,I_v \tag{20}$$

Considering Equation (13) whose solution upon integration is obtained as

$$S_h(t) \geqslant S_h(0)e^{-t(\beta\,\beta_h+\mu_h)} \geqslant 0 \tag{21}$$

and in a similar manner the solutions of Equations (14)–(20) were obtained as

$$E_h(t) \geqslant E_h(0)e^{-t(\beta\,\beta_h+\mu_h)} \geqslant 0$$

$$I_h(t) \geqslant I_h(0)e^{-t(\tau_h+\mu_h+\sigma_h)} \geqslant 0$$

$$R_h(t) \geqslant R_h(0)e^{-t(\omega_h+\mu_h)} \geqslant 0$$

$$L(t) \geqslant L(0)e^{-t(\kappa+\mu_v)} \geqslant 0$$

□

In conclusion, the solutions of the system of differential Equation (1) are both positive and invariant in Φ [23,24]. As a consequence, the solutions are contained in the closed and bounded interval $0 \leqslant N_h(t) \leqslant \frac{\Lambda_h}{\mu_h}$ for the human population and $0 \leqslant N_v(t) \leqslant \frac{\Lambda_v}{\mu_v}$ for the mosquito population. As such, the model is well posed mathematically and epidemiologically well stated.

5. Dengue-free equilibrium

The dengue-free Equilibrium (DFE) state was determined to exist by setting the derivatives on the left-hand side in Equation (1) to zero [25]. At the disease-free equilibrium, dengue fever disease does not exist in the community [26]; therefore,

$I_h(t) = 0$, $E_h(t) = 0$, $I_v(t) = 0$ and $E_v(t) = 0$. As a result, there is no recovery from the disease implying that $R_h(t) = 0$.

The system reduces to the following non-trivial system of equations

$$\begin{aligned} 0 &= \Lambda_h - (\beta\,\beta_h + \mu_h)\,S_h + \omega_h R_h \\ 0 &= \Lambda_v - (\kappa + \mu_v)\,L \\ 0 &= \kappa L - (\beta\,\beta_v + \mu_v)\,S_v \end{aligned}$$

This system of equations was solved to obtain the dengue-free equilibrium state given by

$$\xi_0 = (S_h^*, E_h^*, I_h^*, R_h^*, L^*, S_v^*, E_v^*, I_v^*) = \left(\frac{\Lambda_h}{\mu_h}, 0, 0, 0, \frac{\Lambda_v}{\kappa + \mu_v}, \frac{\Lambda_v}{\mu_v}\left(\frac{\kappa}{\kappa + \mu_v}\right), 0, 0\right) \tag{22}$$

Hence confirming the existence of the Dengue-Free Equilibrium point in the spread dynamics characterised by the system of differential Equation (1).

5.1. The basic reproductive number

The basic reproduction number $\Re_0$ was calculated using the next-generation matrix which requires the heterogeneous population to be divided into infective and non-infective compartments [27, 28]. The infective compartments, which included E_h, I_h, E_v, I_v, were used to determine the matrices F and V, which are necessary in the next-generation matrix scheme. The F and V matrices were given as follows

$$F = \begin{bmatrix} 0 & \frac{\beta_h \Lambda_h}{\mu_h} & 0 & \frac{\beta_h \Lambda_h}{\mu_h} \\ 0 & 0 & 0 & 0 \\ 0 & \frac{\beta_v \kappa \Lambda_v}{\mu_v(\kappa+\mu_v)} & 0 & \frac{\beta_v \kappa \Lambda_v}{\mu_v(\kappa+\mu_v)} \\ 0 & 0 & 0 & 0 \end{bmatrix} \quad \text{and} \quad V = \begin{bmatrix} \alpha_h + \mu_h & 0 & 0 & 0 \\ -\alpha_h & \tau_h + \mu_h + \sigma_h & 0 & 0 \\ 0 & 0 & \tau_v + \mu_v & 0 \\ 0 & 0 & \tau_v & -\mu_v \end{bmatrix}$$

The basic reproduction number $\Re_0$ was determined by the spectral radius of the matrix $F \cdot V^{-1}$ [29,30], which was determined to be

$$\Re_0 = \frac{\Lambda_h\,\mu_v\,\beta_h\,\alpha_1\,(\tau_v + \mu_v)\,\mu_v\,(\kappa + \mu_v) + \beta_v\,\kappa\,\Lambda_v\,\tau_v\,(\alpha_h + \mu_h)\,(\tau_h + \mu_h + \sigma_h)\,\mu_h}{\mu_h\,\mu_v\,\mu_v\,(\kappa + \mu_v)\,(\alpha_1 + \mu_h)\,(\tau_h + \mu_h + \sigma_h)\,(\tau_v + \mu_v)} \tag{23}$$

The basic Reproductive number $\Re_0$ in Equation (23) can be simplified further into

$$\Re_0 = \frac{\beta_v\,\kappa\,\Lambda_v\,\tau_v}{\mu_v\,(\kappa + \mu_v)\,(\tau_v + \mu_v)\,\mu_v} + \frac{\beta_h\,\Lambda_h\,\alpha_h}{\mu_h\,(\alpha_h + \mu_h)\,(\tau_h + \mu_h + \sigma_h)} \tag{24}$$

The Equation (24) implies that the basic reproductive number is a linear combination of the basic reproductive in the mosquito population($\Re_{0v}$) and the basic reproductive number of the human population ($\Re_{0h}$) i.e $\Re_0 = \Re_{0v} + \Re_{0h}$. Where

$$\Re_{0h} = \frac{\beta_v\,\kappa\,\Lambda_v\,\tau_v}{\mu_v\,(\kappa + \mu_v)\,(\tau_v + \mu_v)\,\mu_v} \quad \text{and} \quad \Re_{0v} = \frac{\beta_h\,\Lambda_h\,\alpha_h}{\mu_h\,(\alpha_h + \mu_h)\,(\tau_h + \mu_h + \sigma_h)}$$

5.2. Local stability of the Dengue-Free Equilibrium (DFE)

Theorem 3. *The Dengue-Free Equilibrium* (ξ_0) *is locally asymptotically stable point of the dynamical system 1 whenever* $\Re_0 < 1$.

Proof. In order to prove the local stability of the DFE we need to determine the Jacobian of the non-linear system of differential Equation (1) at the DFE ξ_0 [31]. The DFE is locally stable if the Eigenvalues of the system of the linearised differential equations arising from the system of differential Equation 1 are less than 0 [32]. Linearising the ODE system1 we obtained the Jacobian matrix as

$$\mathscr{J}_{DFE} = \begin{bmatrix} -\beta\,\beta_h - \mu_h & 0 & 0 & 0 & 0 & 0 & 0 & 0 \\ \beta\,\beta_h & -\alpha_h - \mu_h & 0 & 0 & 0 & 0 & 0 & 0 \\ 0 & \alpha_h & -\tau_h - \mu_h - \sigma_h & 0 & 0 & 0 & 0 & 0 \\ 0 & 0 & \tau_h & -\omega_1 - \mu_h & 0 & 0 & 0 & 0 \\ 0 & 0 & 0 & 0 & -\kappa - \mu_v & 0 & 0 & 0 \\ 0 & 0 & 0 & 0 & \kappa & -\beta\,\beta_v - \mu_v & 0 & 0 \\ 0 & 0 & 0 & 0 & 0 & 0 & -\tau_v - \mu_v & 0 \\ 0 & 0 & 0 & 0 & 0 & 0 & \tau_v & -\mu_v \end{bmatrix}$$

Which was evaluated about the DFE $\left(\frac{\Lambda_h}{\mu_h}, 0, 0, 0, \frac{\Lambda_v}{\kappa+\mu_v}, \frac{\Lambda_v}{\mu_v}\left(\frac{\kappa}{\kappa+\mu_v}\right), 0, 0\right)$ we obtained

$$\begin{bmatrix} -\mu_h & 0 & 0 & 0 & 0 & 0 & 0 & 0 \\ 0 & -\alpha_h - \mu_h & 0 & 0 & 0 & 0 & 0 & 0 \\ 0 & \alpha_h & -\tau_h - \mu_h - \sigma_h & 0 & 0 & 0 & 0 & 0 \\ 0 & 0 & \tau_h & -\omega_1 - \mu_h & 0 & 0 & 0 & 0 \\ 0 & 0 & 0 & 0 & -\kappa - \mu_v & 0 & 0 & 0 \\ 0 & 0 & 0 & 0 & \kappa & -\mu_v & 0 & 0 \\ 0 & 0 & 0 & 0 & 0 & 0 & -\tau_v - \mu_v & 0 \\ 0 & 0 & 0 & 0 & 0 & 0 & \tau_2 & -\mu_v \end{bmatrix}$$

The eigenvalues of the linearised system at DFE were given by

$$\begin{bmatrix} -\mu_h \\ -(\omega_1 + \mu_h) \\ -(\alpha_h + \mu_h) \\ -(\tau_h + \mu_h + \sigma_h) \\ -(\tau_v + \mu_v) \\ -(\kappa + \mu_v) \\ -\mu_v, \\ -\mu_v \end{bmatrix}$$

All the Eigenvalues of the systems are less than zero thus the system is locally

asymptotically stable since the solutions will approach zero when $t \to \infty$. As such, $\mathfrak{R}_0$ is guaranteed to be less than one.

5.3. Global stability of the Dengue-Free Equilibrium

Theorem 4. *The Dengue-Free Equilibrium is globally asymptotically stable if the basic reproductive number is less than one in the given interval.*

Proof. We considered the Lyapunov function [33]

$$\mathfrak{V}(t, S_h, E_h, I_h, R_h, L, S_v, E_v, E_v) = C_1 E_h + C_2 I_h + C_3 E_v + C_4 I_v \tag{25}$$

Differentiating the Lyapunov function 25 with respect with respect to time [34] we obtained

$$\frac{\mathrm{d}\mathfrak{V}}{\mathrm{d}t} = C_1 \frac{\mathrm{d}E_h}{\mathrm{d}t} + C_2 \frac{\mathrm{d}I_h}{\mathrm{d}t} + C_3 \frac{\mathrm{d}E_v}{\mathrm{d}t} + C_4 \frac{\mathrm{d}I_v}{\mathrm{d}t}$$

replacing the values of $E_h, I_h, E_v,$ and I_v from 1 we obtained the equation

$$\frac{\mathrm{d}\mathfrak{V}}{\mathrm{d}t} = C_1 \left((I_h + I_v) \beta_h S_h - (\alpha_h + \mu_h) E_h \right) + C_2 \left(\alpha_h E_h - (\tau_h + \mu_h + \sigma_h) I_h \right) + C_3 \left((I_h + I_v) \beta_v S_v - (\tau_2 + \mu_v) E_v \right) + C_4 \left(E_v \tau_v - I_v \mu_v \right)$$

At the Dengue-Free Equilibrium $\xi_0 = \left(S_h^*, E_h^*, I_h^*, R_h^*, L^*, S_v^*, E_v^*, I_v^*\right)$ $= \left(\frac{\Lambda_h}{\mu_h}, 0, 0, 0, \frac{\Lambda_v}{\kappa + \mu_v}, \frac{\Lambda_v}{\mu_v} \left(\frac{\kappa}{\kappa + \mu_v} \right), 0, 0 \right)$ we noted that $S_h \leqslant S_h^*, E_h \leqslant E_h^*, I_h \leqslant I_h^*, R_h \leqslant R_h^*, L \leqslant L^*, S_v \leqslant S_v^*, E_v \leqslant E_v^*, I_v \leqslant I_v^*$. Therefore, we substituted the Dengue-free Endemic equilibrium values for the non-infected compartments and obtained

$$\begin{aligned} \frac{\mathrm{d}\mathfrak{V}}{\mathrm{d}t} \leqslant C_1 \left((I_h + I_v) \beta_h \left(\frac{\Lambda_h}{\mu_h} \right) - (\alpha_h + \mu_h) E_h \right) + C_2 \left(\alpha_h E_h - (\tau_h + \mu_h + \sigma_h) I_h \right) + \\ C_3 \left((I_h + I_v) \beta_v \frac{\Lambda_v}{\mu_v} \left(\frac{\kappa}{\kappa + \mu_v} \right) - (\tau_2 + \mu_v) E_v \right) + C_4 \left(E_v \tau_v - I_v \mu_v \right) \end{aligned} \tag{26}$$

Equation (26) was re-organised to

$$\frac{\mathrm{d}\mathfrak{V}}{\mathrm{d}t} \leqslant \left(C_1 \left(-\alpha_h - \mu_h \right) + C_2 \alpha_h \right) E_h + \left(\frac{C_1 \beta_h \Lambda_h}{\mu_h} + C_2 \left(-\tau_h - \mu_h - \sigma_h \right) + \frac{C_3 \beta_v \kappa \Lambda_v}{\mu_v (\kappa + \mu_v)} \right) I_h \tag{27}$$

$$+ \left(C_3 \left(-\tau_v - \mu_v \right) + C_4 \tau_v \right) E_v + \left(\frac{C_1 \beta_h \Lambda_h}{\mu_h} + \frac{C_3 \beta_v \kappa \Lambda_v}{\mu_v (\kappa + \mu_v)} - C_4 \mu_v \right) I_v \tag{28}$$

Where the constant $C_1, C_2, C_3,$ and C_4, were given as follows

$$\begin{aligned} C_1 &= -\frac{C_2 \alpha_h}{-\alpha_h - \mu_h} \\ C_2 &= 1 \\ C_3 &= \frac{\mu_v (\kappa + \mu_v)}{\beta_v \kappa \Lambda_v} \left(-\frac{C_1 \beta_h \Lambda_h}{\mu_h} - C_2 \left(-\tau_h - \mu_h - \sigma_h \right) \right) \\ C_4 &= -\frac{1}{\mu_v} \left(-\frac{C_1 \beta_h \Lambda_1}{\mu_h} - \frac{C_3 \beta_v \kappa \Lambda_v}{\mu_v (\kappa + \mu_v)} \right) \end{aligned}$$

Equation (28) simplifies to

$$\frac{\mathrm{d}\mathfrak{V}}{\mathrm{d}t} \leqslant \left[\frac{1}{\mathfrak{R}_{0v}} - \frac{1}{\mathfrak{R}_{0h}} \cdot \frac{\beta_h \Lambda_h \alpha_h}{(\tau_h + \mu_h + \sigma_h)\mu_h(\alpha_h + \mu_h)}\right] \frac{(-1)\tau_v(\tau_h + \mu_h + \sigma_h)(\alpha_h + \mu_h)\Lambda_v}{\alpha_h + \mu_h} E_v \leqslant 0 \tag{29}$$

Which implied that $\dfrac{\mathrm{d}\mathfrak{V}}{\mathrm{d}t} = 0$ only when $E_v = 0$. As such, the Dengue-free Equilibrium ξ_0 is globally asymptotically stable when $\mathfrak{R}_{0v} < 1$ based on LaSalle's invariance principle [33,35]. That is, When $\mathfrak{R}_{0v} < 1$ in Equation (29), then $\left[\dfrac{1}{\mathfrak{R}_{0v}} - \dfrac{1}{\mathfrak{R}_{0h}} \cdot P - 1\right]$ will approach $\left[\dfrac{1}{\mathfrak{R}_{0v}} > 1 + \dfrac{1}{\mathfrak{R}_{0h}} \cdot P\right]$ which guarantees global stability. Where $P = \dfrac{\beta_h \Lambda_h \alpha_h}{(\tau_h + \mu_h + \sigma_h)\mu_h(\alpha_h + \mu_h)}$.

6. Numerical analysis and discussions

In this section, we present numerical analysis simulations that illustrate the dynamical behaviours of the systems of the non-linear differential Equation (1).

6.1. Sensitivity indices

Sensitivity analysis was conducted to determine the prominence of each parameter contributing to the basic reproductive number ($\mathfrak{R}_0$), which consequently makes them the most significant drivers of the disease in the spread dynamics [34]. The indices were determined using the normalised forward-sensitivity index method [36], whose results were presented in **Table 2** below.

Table 2. Local Sensitivity indices of the basic reproductive number $\mathfrak{R}_0$.

Parameter	Description	Sensitivity index
Λ_h	Human Recruitment rate.	$0.6781034150 \times 10^{-3}$
τ_h	Human recovery rate.	$-0.8262326545 \times 10^{-4}$
β_h	Infection rate of the susceptible Humans	$0.6781034150 \times 10^{-3}$
α_h	Rate of humans moving from latent stage to infectious stage.	$0.7125629625 \times 10^{-4}$
σ_h	Dengue fever mortality rate.	$-0.5198827545 \times 10^{-3}$
μ_1	Natural death rate of humans.	$-0.8249571056 \times 10^{-3}$
τ_v	Rate of mosquitoes moving from latent stage to infectious stage.	0.2439765474
Λ_v	Egg-laying rates of Aedes aegypti mosquitoes.	0.9993218966
κ	Survival rates of mosquitoes at the pre-development stage.	0.9993218964
β_v	Infection rate of susceptible mosquitoes.	0.9993218966
μ_v	Natural death rate of *Aedes aegypti* mosquitoes.	-1.243298445

6.2. Numerical simulations of the dengue fever spread dynamics

In this subsection, we present graphical illustrations of the dengue fever disease spread dynamics in Kenya. The graphical illustrations are presented to illustrate some of the analytical solutions discussed earlier. The illustrations are based on the system of differential Equation (1) which has been proven to be both mathematically well-stated

and epidemiologically well-posed.

The numerical values of the parameters utilised in the graphical simulations were summarised in **Table 2**. They were used together with the following initial conditions $S(0) = 99999, E_h = 100, I_h = 10, R_h = 0, L(0) = 900, S_v = 900, E_v = 10, I_v = 10$. Consequently, the combined dengue fever spread dynamics trends were illustrated in **Figure 3** below.

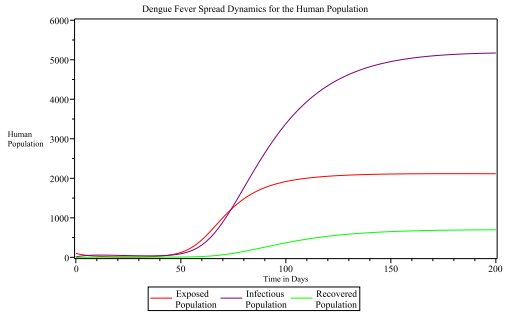

(a) Dengue fever spread dynamics among the human population.

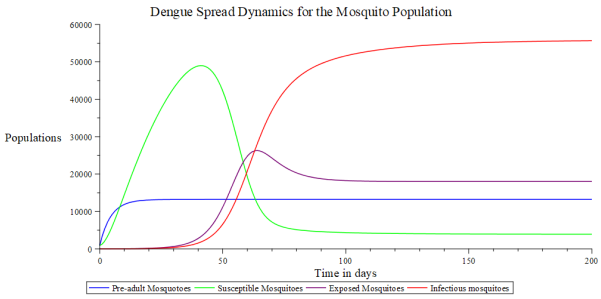

(b) Dengue fever spread dynamics in the mosquito population.

Figure 3. General Dengue fever spread dynamics.

The study further investigated the impact of some sensitive parameters on the spread dynamics of the exposed and infected human beings and the exposed and infected mosquitoes. An increase in the infection rate of mosquitoes denoted by β_v leads to an increased number of exposed and infectious populations of both human beings and mosquitoes. These dynamics are illustrated in **Figure 4** below.

The rate at which mosquitoes survive the pre-adult stage, denoted by κ, also has a directly proportional impact on the basic reproduction number $\Re_0$. When κ decreases, both exposed and infected populations of human beings and mosquitoes decrease with a proportional margin as illustrated in **Figure 5**.

As such, control measures targeting these two parameters can effectively contain the spread dynamics of dengue fever in Kenya.

7. Conclusions and recommendation

Dengue fever is an emerging disease in Kenya that is occasioned by climate change and its impact. To understand its spread dynamics in the country, a new mathematical model has been developed that entails the intrinsic incubation period and the extrinsic incubation period in the form of the exposed mosquito compartment and the exposed human population compartment. The basic properties of the disease spread dynamics have been explored through the determination of the invariant and bounded region. The solutions to the system of differential equations representing the mathematical model have been established to be positive. As such, the model was shown to be both epidemiologically well-stated and mathematically well-posed. The basic reproduction number was determined using the next-generation matrix. It was used to establish the existence of dengue-free equilibrium and the endemic equilibrium. The local and global stabilities of the dengue-free equilibrium were established. The

sensitivity indices of the parameters making up the basic reproduction number ($\Re_0$) were determined using the normalised forward-sensitivity index method. It was established that $\beta_v, \kappa, \mu_v, \tau_v$ and Λ_v were the most sensitive parameters of the basic reproduction number, $\Re_0$. Numerical results of the system of differential equations arising from the dengue fever spread dynamics in Kenya were presented to illustrate the trend of the spread dynamics.

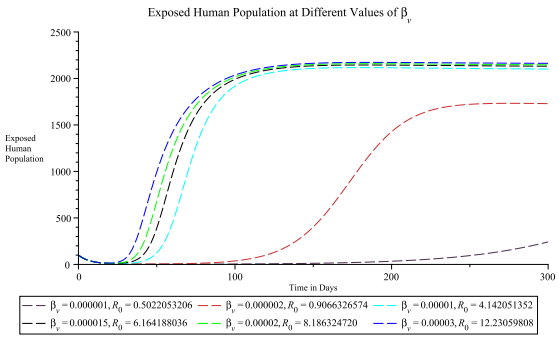

(a) Exposed human population at different values of the infection rates of susceptible mosquitoes β_v.

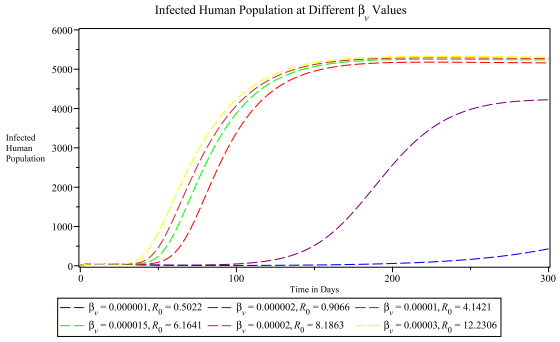

(b) Infected human population at different values of the infection rates of susceptible mosquitoes β_v.

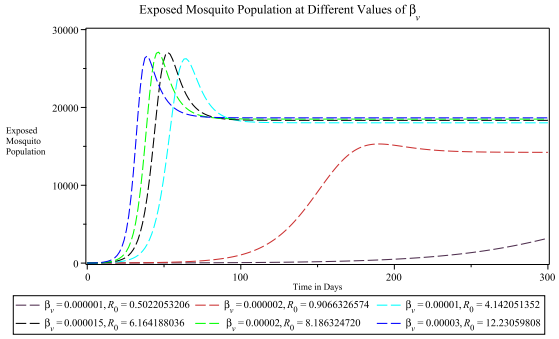

(c) Exposed mosquito population at different values of the infection rates of susceptible mosquitoes β_v.

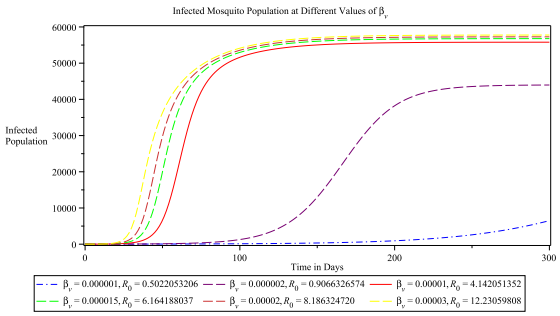

(d) Infected mosquito population at different values of the infection rates of susceptible mosquitoes β_v.

Figure 4. Impact of infection rate of susceptible mosquitoes (β_v) on infective compartments.

The study recommended that control measures be instituted on the most sensitive parameters as established by the sensitivity analysis. The control measures to be implemented should be aimed at containing the spread of dengue fever in Kenya. Furthermore, the mathematical epidemiological model can be expanded by including new compartments that investigate other aspects of the spread dynamics such as misdiagnosis. The impact of climate change on the driving factors of dengue fever spread dynamics can also be explored to determine their influence on dengue fever spread dynamics in Kenya.

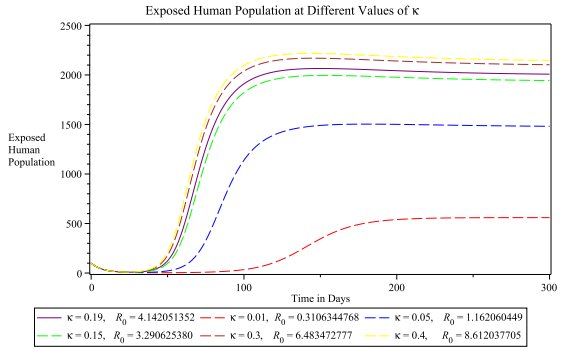

(a) Exposed human population at different values of the survival rates of mosquitoes at the pre-development stage κ.

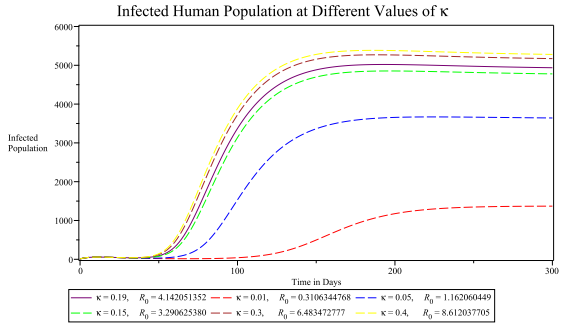

(b) Infected human population at different values of the survival rates of mosquitoes at the pre-development stage κ.

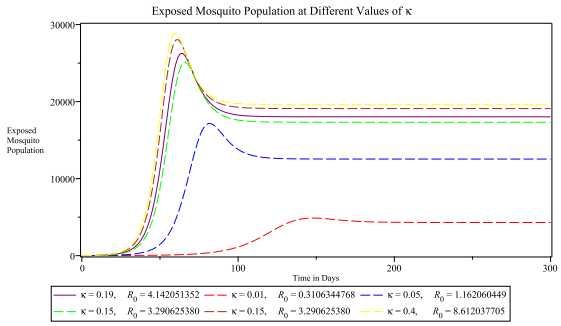

(c) Exposed mosquito population at different values of the survival rates of mosquitoes at the pre-development stage κ.

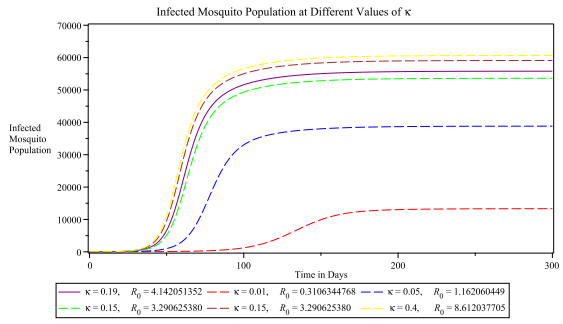

(d) Infected mosquito population at different values of the survival rates of mosquitoes at the pre-development stage κ.

Figure 5. Impact of the survival rates of mosquitoes at the pre-development stage (κ) on the infective compartments.

Author contributions: Conceptualization, BN and YY; methodology, BN; software, BN; validation, GK , MW and BN; formal analysis, BN; investigation, BN; resources, BN; data curation, BN; writing—original draft preparation, BN; writing—review and editing, BN; visualization, BN; supervision, GK and MW; project administration, MW. All authors have read and agreed to the published version of the manuscript.

Conflict of interest: The authors declare no conflict of interest.

References

1. Gubler DJ. Dengue, urbanization and globalization: the unholy trinity of the 21st century. Tropical medicine and health. 2011; 39(4SUPPLEMENT): S3–S11,
2. Khan NT. Etiology of dengue fever. Open Access Journal of Biomedical Science. 2022; 4(2).
3. Yue Y, Liu X, Ren D, et al. Spatial dynamics of dengue fever in mainland china, 2019. International Journal of Environmental Research and Public Health. 2021: 18(6): 2855.
4. Guzman MG, Harris E. Dengue. The Lancet. 2015; 385(9966): 453–465.
5. Wu T, Wu Z, Li YP. Dengue fever and dengue virus in the people's republic of china. Reviews in Medical Virology. 2022; 32(1): e2245.
6. Kothai R, Arul B. Dengue fever: An overview. Dengue Fever. 2020.
7. Cogan JE. Dengue and severe dengue. Available online: http://www. who. int/en/news-room/fact-sheets/detail/dengue

-and-severe-dengue (accessed on 2 June 2024).
8. Medagama A, Dalugama C, Meiyalakan G, et al. Risk factors associated with fatal dengue hemorrhagic fever in adults: A case control study. Canadian Journal of Infectious Diseases and Medical Microbiology. 2020.
9. Martin E, Chirivella M, Co JKG, et al. Insights into the molecular evolution of dengue virus type 4 in Puerto Rico over two decades of emergence. Virus Research. 2016; 213: 23–31.
10. Khetarpal N, Khanna I. Dengue fever: Causes, complications, and vaccine strategies. Journal of immunology research. 2016; 2016: 6803098
11. Deng SQ, Yang X, Wei Y, et al. A review on dengue vaccine development. Vaccines. 2020; 8(1): 63.
12. Bosire C, Mutuku F, Ndenga B, et al. A narrative review of dengue fever infection and epidemic activity in Kenya (2010 to 2020). 2023; 12(10).
13. Konongoi L, Ofula V, Nyunja A, et al. Detection of dengue virus serotypes 1, 2 and 3 in selected regions of Kenya: 2011–2014. Virology Journal. 2016; 13(1): 1–11.
14. Kamau E, Luka MM, de Laurent ZR, et al. Genome sequences of human coronavirus OC43 and NL63, associated with respiratory infections in Kilifi, Kenya. Microbiology Resource Announcements. 2019; 8(46): e00730–19.
15. Obonyo M, Fidhow A, Ofula V. Investigation of laboratory confirmed Dengue outbreak in North-eastern Kenya, 2011. PloS One. 2018; 13(6): e0198556.
16. Attaway DF, Jacobsen KH, Falconer A, et al. Mosquito habitat and dengue risk potential in kenya: Alternative methods to traditional risk mapping techniques. Geospatial Health. 2014; 9(1): 119–130.
17. Muthanje EM, Kimita G, Nyataya JN, et al. March 2019 dengue fever outbreak at the Kenyan south coast involving dengue virus serotype 3, genotypes III and V. PLOS Global Public Health. 2022; 2(3): e0000122.
18. Pollett S, Gathii K, Figueroa K, et al. The evolution of dengue-2 viruses in Malindi, Kenya and greater East Africa: Epidemiological and immunological implications. Infection, Genetics and Evolution. 2021; 90: 104617.
19. Asamoah, JKK, Yankson E, Okyere E, et al. Optimal control and cost-effectiveness analysis for dengue fever model with asymptomatic and partial immune individuals. Results in Physics. 2021; 104919: 31.
20. Kretzschmar M. Disease modeling for public health: added value, challenges, and institutional constraints. Journal of public health policy. 2020; 41: 39–51.
21. Khan MA. Dengue infection modeling and its optimal control analysis in East Java, Indonesia. 2021; 7(1): e06023.
22. Zou L, Chen J, Feng X, Ruan S. Analysis of a dengue model with vertical transmission and application to the 2014 dengue outbreak in Guangdong Province, China. Bulletin of Mathematical Biology. 2018; 80: 2633–2651.
23. Nyasagare BN, Osman S, Wainaina M. Modelling and analysis of campylobacteriosis in human and animal populations, glob. J. Pure Appl. Math. 2019; 15(5): 551–567.
24. Onsongo WM, Mwini ED, Nyanaro BN, et al. Stability analysis and modelling the dynamics of psittacosis in human and poultry populations. Commun. Math. Biol. Neurosci. 2022.
25. Eyaran WE, Osman S, Wainaina M. Modelling and analysis of seir with delay differential equation. Global Journal of Pure and Applied Mathematics. 2019; 15(4): 365–382.
26. Onsongo WM, Mwini ED, Nyanaro BN, Osman S. The dynamics of psittacosis in human and poultry populations: a mathematical modelling perspective. J. Math. Comput. Sci. 2021; 11(6): 8472–8505.
27. Zhang T, Dong C, Wang X. Dynamics analysis of a stochastic SIRVI epidemic model with weak immunity. Applied Mathematics Letters. 2024; 149: 108898.
28. Diekmann O, Heesterbeek JAP, Metz JAJ. On the definition and the computation of the basic reproduction ratio R 0 in models for infectious diseases in heterogeneous populations. Journal of Mathematical Biology. 1990; 28: 365–382.
29. Van den Driessche P, Watmough J. Reproduction numbers and sub-threshold endemic equilibria for compartmental models of disease transmission. Mathematical Biosciences. 2002; 180(1-2): 29–48.
30. Muia DW, Osman S, Wainaina M. Modelling and analysis of trypanosomiasis transmission mechanism. Global Journal of Pure and Applied Mathematics. 2018; 14(10): 1311–1331.
31. Osman S, Otoo D, Sebil C. Analysis of listeriosis transmission dynamics with optimal control. Applied Mathematics. 2020; 11(7): 712–737.
32. Osman S, Otoo D, Daniel Makinde O. Modeling anthrax with optimal control and cost effectiveness analysis. Applied Mathematics. 2020; 11(3): 255–275.
33. Ito H. Input-to-state stability and Lyapunov functions with explicit domains for SIR model of infectious diseases. Discrete and Continuous Dynamical Systems-Series B. 2021; 26: 9.
34. Osman S, Daniel Makinde O. A mathematical model for coinfection of listeriosis and anthrax diseases. International Journal of Mathematics and Mathematical Sciences. 2018; 1: 1725671.

35. Theuri DM. Stability analysis and modelling of listeriosis dynamics in human and animal populations. Global Journal of Pure and Applied MatheMatics. 2018; 14(1): 115–138.
36. Anthony Eustace K, Osman S, Wainaina M. Mathematical modelling and analysis of the dynamics of cholera. Global Journal of Pure and Applied Mathematics. 2018; 14(9): 1259–1275.